Journal of Neurocytology **28**, 333–347 (1999)

Myelinating Schwann cells determine the internodal localization of Kv1.1, Kv1.2, Kv 2, and Caspr

EDGARDO J. ARROYO[1], YI-TIAN XU[1], LEI ZHOU[2], ALBEE MESSING[3], ELIOR PELES[4], SHING YAN CHIU[2], and STEVEN S. SCHERER

[1] *Department of Neurology, The University of Pennsylvania Medical Center, USA;* [2] *Dept. of Physiology, The University of Wisconsin, 1300 University Ave., Room 285 Medical Science Bldg., Madison, WI 53706, USA;* [3] *Department of Pathobiological Sciences, School of Veterinary Medicine, The University of Wisconsin-Madison, Madison, WI 53706, USA;* [4] *Department of Molecular Cell Biology, Weizmann Institute of Science, 76100 Rehovot, Israel*

Summary

We examined the localization of Caspr and the K^+ channels Kv1.1 and Kv1.2, all of which are intrinsic membrane proteins of myelinated axons in the PNS. Caspr is localized to the paranode; Kv1.1, Kv1.2 and their 2 subunit are localized to the juxtaparanode. Throughout the internodal region, a strand of Caspr staining is flanked by a double strand of Kv1.1/ Kv1.2/Kv 2 staining. This tripartite strand apposes the inner mesaxon of the myelin sheath, and forms a circumferential ring that apposes the innermost aspect of Schmidt-Lanterman incisures. The localization of Caspr and Kv1.2 are not disrupted in mice with null mutations of the myelin associated glycoprotein, connexin32, or Kv1.1 genes. At all of these locations, Caspr and Kv1.1/ Kv1.2/Kv 2 define distinct but interrelated domains of the axonal membrane that appear to be organized by the myelin sheath.

Introduction

Myelin is an important vertebrate adaptation, and is found in the CNS and PNS of all jawed vertebrates. By restricting sodium currents to nodes of Ranvier and reducing the capacitance of the internodal axonal membrane, myelin facilitates saltatory conduction, thereby greatly increasing conduction velocity. The molecular architecture of axons and their myelin sheaths are specialized for this function, having similar structural features in the CNS and PNS (Peters *et al.*, 1991; Berthold & Rydmark, 1995; Hirano & Llena, 1995). The nodal axonal membrane is highly enriched in voltage-sensitive Na^+ channels that allow the Na^+ to depolarize the axon (Shrager & Wu, 1994). The paranodal axonal membrane contains contactin-associated protein (Caspr) (Einheber *et al.*, 1997; Peles *et al.*, 1997), also known as paranodin (Menegoz *et al.*, 1997), a putative cell adhesion molecule that may link the axonal and glial membranes. The juxtaparanodal axonal membrane contains two *Shaker* type K^+ channels, Kv1.1 and Kv1.2, and their associated 2 subunit, Kv 2 (Wang *et al.*, 1993; Mi *et al.*, 1995; Rhodes *et al.*, 1997; Rasband *et al.*, 1998; Vabnick & Shrager, 1998; Vabnick *et al.*, 1999). The analysis of *Kv1.1*-null mice (Smart *et al.*, 1998) reveals a novel role for Kv1.1 in preventing re-excitation of myelinated fibers, which fits with the delayed rectifying properties of these channels (Zhou *et al.*, 1998; Chiu *et al.*, 1999).

The molecular architecture of myelinated fibers arises during development by a stepwise specialization of the axonal and glial membranes, best described in the PNS (Rosenbluth, 1988; Bennett *et al.*, 1997). Myelinating Schwann cells initially ensheathe an axon in a 1 : 1 manner, and express periaxin and myelin-associated glycoprotein (MAG) on their adaxonal surface, which apposes the axon (Trapp & Quarles, 1982; Martini & Schachner, 1988; Gillespie *et al.*, 1994). As the inner mesaxon continues to spiral around the axon, the adjacent layers of Schwann cell membrane become tightly apposed, forming compact myelin, which is highly enriched in protein zero (P_0), myelin-basic protein (MBP), and peripheral myelin protein 22 kDa (PMP22). Shortly after compact myelin is formed, Schmidt-Lanterman incisures appear, which are funnel-shaped regions of non-compact myelin within the compact myelin (Friede & Samorajski, 1969; Small *et al.*, 1987). Incisures contain a unique set of specializations, including adherens junctions and gap junctions, which are also found

To whom correspondence should be addressed.

0300–4864

in paranodes but not in compact myelin (Scherer, 1996). Adherens junctions contain E-cadherin, - and -catenin (Fannon *et al.*, 1995) and the gap junctions are composed of connexin32 (Cx32) and perhaps other connexins (Balice-Gordon *et al.*, 1998).

The axonal membrane also undergoes a sequential transformation during development. In the PNS, the cell adhesion molecules (CAMs) Nr-CAM and neurofascin are the first molecules to appear at prospective nodes, followed by ankyrin$_G$ isoforms and voltage-dependent Na^+ channels (Lambert *et al.*, 1997). Clusters of Kv1.1, Kv1.2 and Kv 2 appear after clusters of Na^+ channels and ankyrin$_G$ are well established (Vabnick & Shrager, 1998; Vabnick *et al.*, 1999). These K^+ channels gradually become sequestered in the juxtaparanodal region, where they are thought to be electrically isolated from the nodes. In myelinating co-cultures, Caspr and contactin are initially uniformly distributed along the axonal membrane; contactin disappears as axons are ensheathed and myelinated by Schwann cells, whereas Caspr becomes highly concentrated at paranodes (Einheber *et al.*, 1997). The molecular maturation of the paranodal region is accompanied by a striking increase in the axonal conduction velocity and progressively diminishing effects of K^+ channel blockers (Vabnick *et al.*, 1999).

A lively debate has developed regarding whether Schwann cells or axons specify the locations of the structural and molecular specializations in the nodal region (Salzer, 1997). Here we report that the paranodal and internodal distributions of Caspr, Kv1.1, and Kv1.2 are intricately related to the structure of the overlying myelin sheath. The most parsimonious explanation for their precise localization is that the myelin sheath organizes them; the converse seems unlikely. These data provide strong evidence that myelin sheath organizes the underlying axonal membrane and provide further evidence for a central role of Schwann cells in the development of axonal specializations.

Materials and Methods

Mag-null (Li *et al.*, 1994) mice were obtained from Jackson Laboratories; *cx32*-null mice were obtained from Prof. Klaus Willecke (Nelles *et al.*, 1996). The generation of *Kv1.1*-null mice has been described (Smart *et al.*, 1998).

Teased nerve fibers were prepared from adult mouse and rat sciatic nerves, either from unfixed nerves, or after fixation for 30–60 minutes in freshly prepared 4% paraformaldehyde (in 0.1 M phosphate buffer pH 7.4) or Zamboni's fixative (Zamboni & de Martino, 1967). Fibers were dried on glass slides (Fisher SuperFrost Plus) overnight at room temperature and stored at -20°C. Fibers were post-fixed and permeabilized by immersion in -20°C acetone for 10 minutes, blocked at room temperature for at least 1 hour in 5% fish skin gelatin containing 0.1% tritonX100 in PBS, and incubated 24–48 hours at 4°C with various combinations of primary antibodies. We used rabbit antisera against rat Kv1.1 and Kv1.2 (Alomone Labs; Jerusalem, Israel), Caspr (Einheber *et al.*, 1997; Peles *et al.*, 1997), MAG (Pedraza *et al.*, 1990), Cx32 (Chemicon; Temecula, CA) and nodal Na^+ channels (Vabnick *et al.*, 1997), and in various combinations with mouse monoclonal antibodies against rat MAG (513, diluted 1:100, Boehringer Mannheim), Cx32 (Scherer *et al.*, 1998), ankyrin$_G$ (diluted 1:100; Zymed, South San Francisco, CA), Kv1.1 and Kv1.2 (diluted 1:100; Upstate Biotechnology, Lake Placid, NY), Kv 1 and Kv 2 (diluted 1:100; (Rhodes *et al.*, 1997), and a rat monoclonal antibody against neurofilament heavy (Ta51, diluted 1:10; (Lee *et al.*, 1982). After incubating with the primary antibodies, the slides were washed, incubated with the appropriate fluorescein- , rhodamine, and cyanine 5-conjugated donkey anti-rabbit and/or anti-mouse cross-affinity purified secondary antibodies (diluted 1:100; Jackson ImmunoResearch Laboratories, West Grove, PA), and mounted with Vectashield (Vector Laboratories, Inc., Burlingame, CA). Specimens were examined by epifluorescence with TRITC and FITC optics on a Leica DMR light microscope and photographed on Kodak film (ASA 400) or with a Leica TCS laser scanning confocal microscope followed by image manipulation with Adobe Photoshop.

Results

IMMUNOLABELING TEASED FIBERS

To evaluate the molecular architecture of the paranode, we first examined the localization of Kv1.1, Kv1.2, and Caspr in normal myelinated fibers. Teased fibers were better than cryosections for this analysis, as many details could be better appreciated by following the same fiber. To determine the optimal fixation conditions for every antibody described below, teased fibers were prepared from adult mouse and rat sciatic nerves, from at least three different conditions—unfixed, or fixed in 4% paraformaldehyde or Zamboni's fixative for 30 to 60 minutes. Nerves fixed in paraformaldehyde or Zamboni's had superior structural preservation and more refined localization of antigens. Rabbit antisera against Kv1.1, Kv1.2, Caspr, MAG, Cx32, or Na^+ channels were combined with mouse monoclonal antibodies against Kv1.1, Kv1.2, Kv 1, Kv 2, Cx32, MAG, or ankyrin$_G$, and a rat monoclonal antibody against the neurofilament heavy subunit (NF-H). All of these antibodies have been well characterized (see Materials and Methods). As an additional control, we determined that the rabbit antiserum and mouse monoclonal antibodies against Kv1.1, Kv1.2, Cx32, and MAG did not stain teased fibers from *Kv1.1-*, *Kv1.2-*, *cx32-* or *Mag*-null mice, respectively (Fig. 7 and data not shown). Further, the Kv1.1 and Kv1.2 antibodies labeled teased fibers from *kv1.2-* and *kv1.1*-null mice, respectively, further demonstrating the selectivity of these antibodies (data not shown). The rabbit antisera robustly stained both mouse and rat teased fibers, but the mouse monoclonal antibodies typically did not label mouse teased fibers as well as those from rats—the signals were higher and/or the backgrounds were lower (endogenous mouse immunoglobulins probably cause the high

background). Thus, optimal labeling was achieved in rat tissues, but comparable results were obtained in mouse tissues.

THE PARANODAL AND INTERNODAL LOCALIZATION OF Kv1.1, Kv1.2, AND Kv 2 IN THE PNS

We compared the localization of voltage-dependent Na^+ channels to those of delayed rectifying K^+ channels, Kv1.1 and Kv1.2, and their associated subunits, Kv 1 and Kv 2. As shown in Figure 1A and B, voltage-dependent Na^+ channels were localized to nodes, whereas both Kv1.1 and Kv1.2 were highly enriched in the juxtaparanodal region, which is immediately adjacent to the paranodal region, as previously shown by others (Ellisman & Levinson, 1982; Haimovich *et al.*, 1984; Wang *et al.*, 1993; Mi *et al.*, 1995; Rhodes *et al.*, 1997; Rasband *et al.*, 1998; Vabnick & Shrager, 1998; Vabnick *et al.*, 1999). To determine whether Kv1.1 and Kv1.2 were always co-localized, we examined teased rat fibers that had been stained with rabbit Kv1.1 and mouse Kv1.2. More than 100 nodes were examined, and in every case, the juxtaparanodal regions were double-labeled; the staining was typically identical even in intricate details (Fig. 1C and D). Similar results were obtained after double-labeling with mouse Kv1.1 and rabbit Kv1.2 antibodies (Fig. 1E and F; (Rasband *et al.*, 1998). Faint Kv1.1- and Kv1.2-immunoreactivity was seen in the perinuclear cytoplasm of myelinating Schwann cells (data not shown), perhaps reflecting their expression of these genes (Chiu *et al.*, 1994). Kv 2 was co-localized with Kv1.1 and Kv1.2 in the juxtaparanodal region (Fig. 1G and H), whereas the Kv 1 antibody did not stain myelinated axons (Rhodes *et al.*, 1997; Rasband *et al.*, 1998). Kv 1-immunoreactivity was seen in cellular cords, probably in unmyelinated axons and/or their associated non-myelinating Schwann cells (data not shown).

In addition to the prominent juxtaparanodal staining, we noted a previously undescribed pattern of internodal staining for Kv1.1, Kv1.2, and Kv 2. A strand of immunoreactivity extended between the two juxtaparanodal regions (Fig. 1C–H, Fig. 2A–H). In many cases, this strand could be resolved into a pair of closely spaced strands running in parallel (Fig. 1E and F, Fig. 2A, C and E). We considered the possibility that this double strand was related to the inner mesaxon, so we labeled teased fibers with rabbit antisera against either Kv1.1 or Kv1.2 and a mouse monoclonal antibody against MAG. MAG is also localized around the entire adaxonal surface of myelinating Schwann cells, and is particularly enriched at the inner mesaxon (Trapp & Quarles, 1982; Martini & Schachner, 1988). Although the MAG staining at inner mesaxons was only seen in a minority of fibers, presumably for technical reasons, when present, it colocalized with the strand of Kv1.1- and Kv1.2-immunoreactivity (Fig. 2A–F).

The fibers that were double-labeled for MAG and Kv1.1 or 1.2 also provided evidence that the Kv1.1 and Kv1.2 labeling was on the axonal membrane. Teasing occasionally broke myelin sheaths and pulled them off their axons. Such denuded axons lacked adaxonal MAG staining, but typically had Kv1.1/Kv1.2 staining, indicating that Kv1.1 and Kv1.2 (and Caspr) were components of axonal, and not Schwann cell, membranes. We also tried to demonstrate this in transverse sections of nerves, but too few fibers were labeled to allow a definite analysis. Immuno-electron microscopy will be required to settle this issue.

Another conspicuous feature of myelinated axons labeled with Kv1.1 or Kv1.2 were circumferential "rings'' along the internodes (Figs. 1 and 2). Like the strands of Kv1.1 and Kv1.2 staining, some of these rings could be shown to be comprised of two, parallel rings (Fig. 1E and F; Fig. 2C and E; Fig. 4). Further, the locations of these rings coincided with incisures, visualized by immunostaining for MAG (Fig. 2C–F), E-cadherin (data not shown), or Cx32 (data not shown). As shown in Fig. 2, incisures are funnel-shaped, and the smallest diameter of the funnel, which is closest to the axon, was in register with the double ring of Kv1.1/Kv1.2 staining. Thus, the internodal distribution of Kv1.1 and Kv1.2, two intrinsic membrane proteins of axons, as well as their Kv 2 subunit, appear to be spatially organized by the myelin sheath.

THE PARANODAL AND INTERNODAL LOCALIZATION OF CASPR IN THE PNS

We also examined the distribution of Caspr-immunoreactivity. As previously reported, Caspr was highly concentrated at paranodes (Einheber *et al.*, 1997; Menegoz *et al.*, 1997). Double-labeling confirmed that Caspr-immunoreactivity apposed MAG- (Fig. 3A and B), E-cadherin- (data not shown), and Cx32-immunoreactivity (data not shown) at paranodes, and did not overlap with Kv1.1 and Kv1.2 at juxtaparanodes (Fig. 3E–H). In addition to the prominent paranodal staining, the internodal region of myelinated axons had a single strand of Caspr-immunoreactivity, sometimes extending from paranode to paranode, but usually ending close to the paranodal region, presumably owing to technical problems that limited more complete labeling. This internodal staining was previously noted by Menegoz *et al.* (1997), who suggested that this strand corresponds to the inner mesaxon. We attempted to show this directly, but only obtained short stretches of Caspr- and MAG-double-labeling of the mesaxon (data not shown). We could readily establish that the occasional circumferential bands of Caspr staining co-localized with MAG-positive incisures, however, since incisures were typically well labeled by the MAG antibody (Fig. 3C and D).

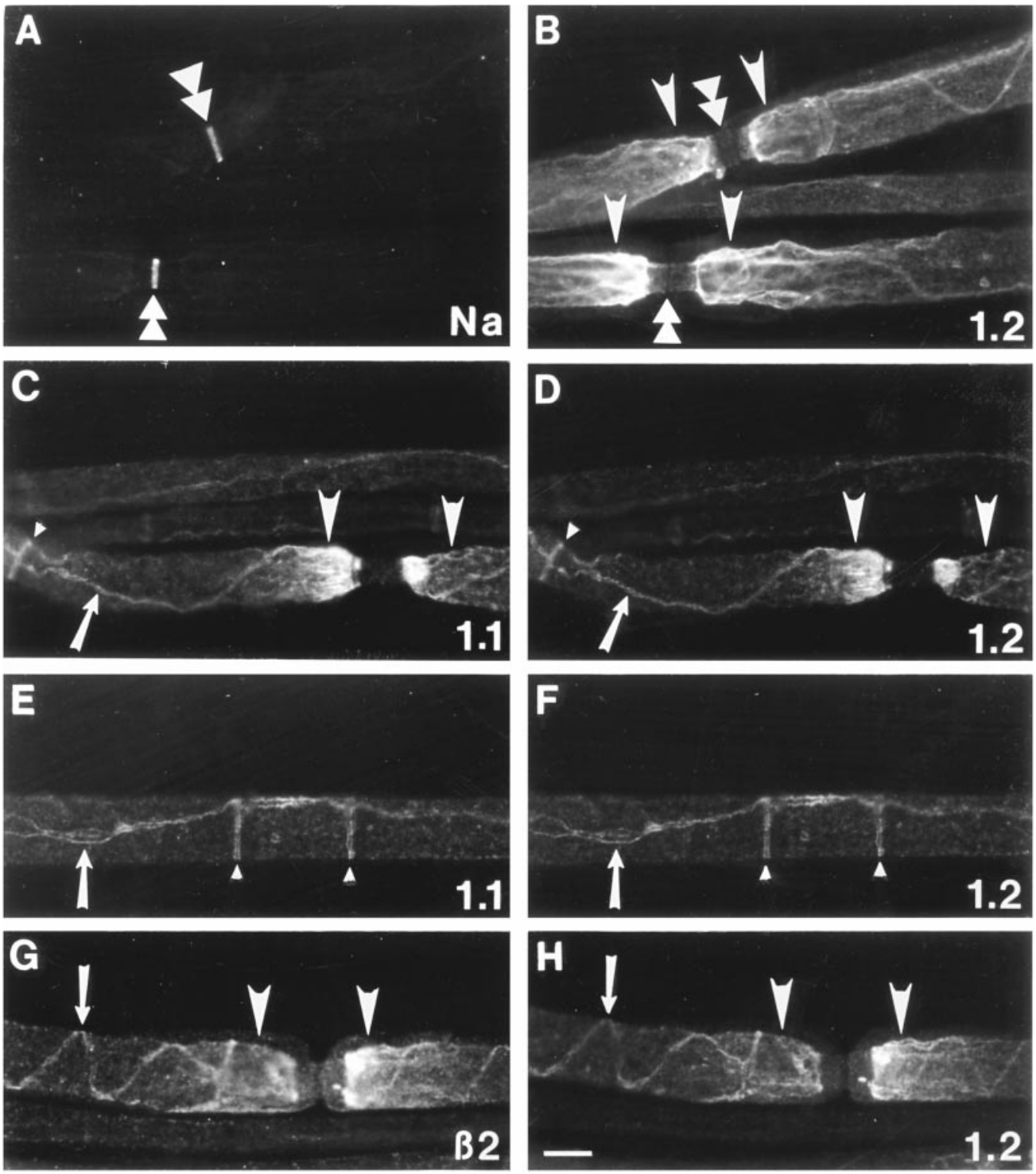

Fig. 1. Kv1.1, Kv1.2, and Kv 2 are co-localized in myelinated fibers and have a non-overlapping distribution with voltage-dependent Na^+ channels. These are photomicrographs of teased fibers from adult rat sciatic nerves, fixed in paraformaldehyde for 30 minutes. The fibers were labeled with rabbit antisera against voltage-dependent Na^+ channels (A), Kv1.1 (C), and Kv1.2 (F and H), and mouse monoclonal antibodies against Kv1.2 (B and D), Kv1.1 (E), and Kv 2 (G), and visualized in TRITC and FITC optics, respectively. Note that Na^+ channels are localized to nodes (double arrowheads), whereas Kv1.1, Kv1.2, and Kv 2 are identically localized at juxtaparanodes (large arrowheads), incisures (small arrowheads), and the inner mesaxon (small arrows). A double line of Kv1.1/Kv1.2 staining is indicated (arrows; E and F). Scale bar: 10 m.

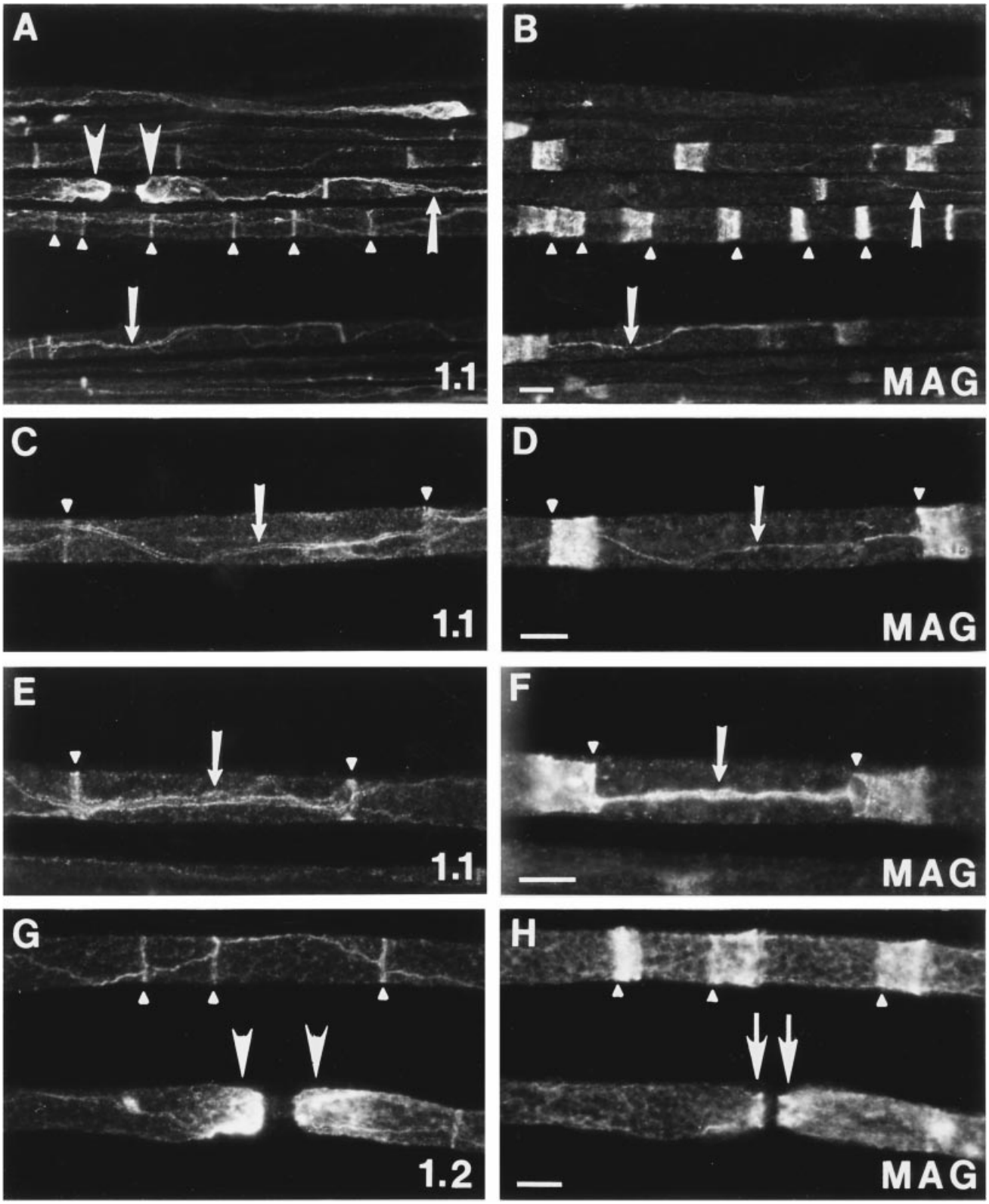

Fig. 2. The paranodal and internodal staining of Kv1.1 and Kv1.2 relate to specializations of the myelin sheath. These are photomicrographs of teased fibers from adult rat (A–F) and mouse (G and H) sciatic nerves, fixed in paraformaldehyde for 30 minutes, and labeled with rabbit antisera against Kv1.1 or Kv1.2 and a mouse monoclonal antibody against MAG, and visualized in TRITC and FITC optics, respectively. Note that Kv1.1- and Kv1.2-immunoreactivity colocalize with MAG-immunoreactivity in the corresponding fields at the inner aspect of incisures (small arrowheads) and at the inner mesaxon (small arrows), but not at juxtaparanodes (large arrowheads). In Panels A, C and E, note the double strand of the Kv1.1 staining (small arrows). Scale bars: 10 m.

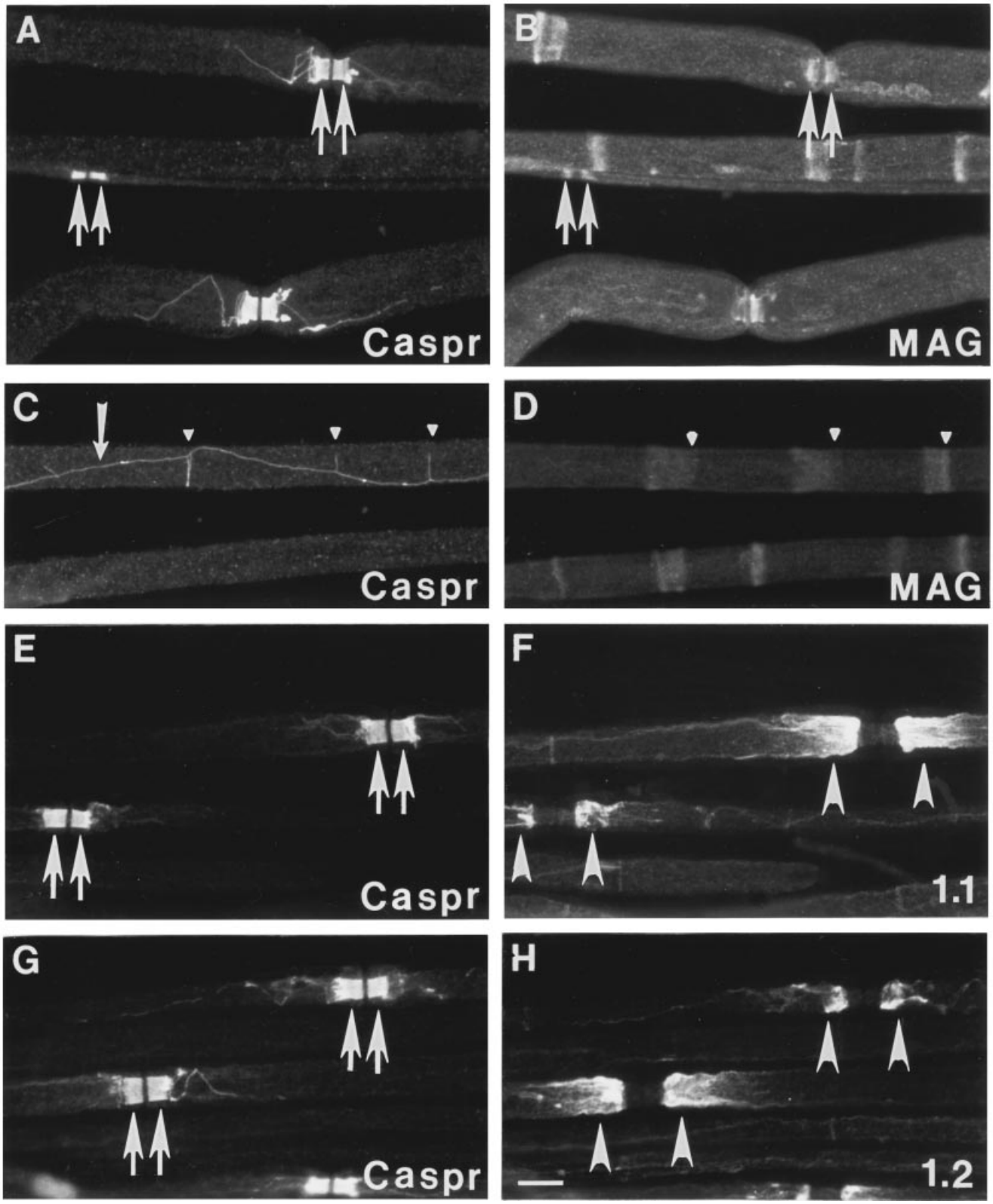

Fig. 3. The localization of Caspr relates to specializations of the myelin sheath, and does not overlap with those of Kv1.1 and Kv1.2. These are photomicrographs of teased fibers from adult mouse sciatic nerves, fixed Zamboni's fixative for 30 minutes, labeled with a rabbit antiserum against Caspr and a mouse monoclonal antibody against MAG, Kv1.1, or Kv1.2, and visualized in TRITC and FITC optics, respectively. In panels A–D, note the broad band of Caspr-immunoreactivity apposing the MAG-immunoreactivity of the myelin sheath at paranodes (large arrows), rings of Caspr staining apposing the inner aspect of MAG staining at incisures (small arrowheads), and a single strand of Caspr staining along the internode (small arrow). In panels E–H, note the Caspr-immunoreactivity in the paranodal region does not overlap with the Kv1.1/Kv1.2-immunoreactivity in the juxtaparanodal region. Scale bar: 10 m.

The above results show that Caspr and Kv1.1/Kv1.2/Kv 2 have closely related but distinct patterns of staining along internodes. We considered the possibility that the single strand of Caspr staining is sandwiched between the double strand of Kv1.1/Kv1.2/Kv 2. As shown in Fig. 4, this proved to be the case. Confocal analysis of triple-labeled teased mouse and rat fibers (rabbit anti-Caspr, mouse anti-Kv1.1 antibodies, and rat anti-NF-H) demonstrated that Caspr is flanked by Kv1.1 along internodes and at incisures. In addition, we noted that NF-H staining was reduced at incisures, just as it is at nodes (Fig. 5). The lack of NF-H staining probably results from the local dephosphorylation of NF-H; this is known to occur at nodes (Mata *et al.*, 1992), but has not previously been noted at incisures.

Another finding not previously emphasized was a spiral of Caspr-immunoreactivity in the juxtaparanodal region. These spirals were typically seen in large, but not small axons, particularly in mice (Fig. 3A). Both paranodes of a given myelin sheath had similarly developed spirals, which had, moreover, a complementary chirality, as might be expected if Caspr apposed the inner mesaxon of the myelin sheath as it spiraled around the axon beyond the confines of the paranodal region (Fig. 8). Further, we noticed an absence of Kv1.1 and Kv1.2 staining in exactly the location of the Caspr-immunoreactivity. This is shown in Fig. 5, by confocal analysis of a teased mouse fiber that was triple-labeled with rabbit anti-Caspr, mouse anti-Kv1.1, and rat anti-NF-H antibodies.

CASPR, Kv1.1 AND Kv1.2 STAINING OF Mag-, cx32-, Kv1.1-NULL MICE

The availability of mutant mice with mutations in myelin-related genes provided an opportunity to explore further the relationship between the myelin sheath and the localization of Caspr, Kv1.1, and Kv.1.2 in the axonal membrane. We were particularly interested in the *Mag*-null mice, as MAG is localized to incisures and the inner mesaxon of the myelin sheath, and has a large extracellular domain that could potentially bind a ligand on the axonal membrane. Moreover, *Mag*-null mice have a diminished periaxonal space and altered neurofilament packing, indicating that the axonal cytoskeleton is altered by the absence of MAG (Li *et al.*, 1994; Montag *et al.*, 1994; Li *et al.*, 1998; Yin *et al.*, 1998). We also examined *cx32*-null mice, as Cx32 is also localized to incisures and the inner mesaxon. In teased fibers from young adult *Mag*- and *cx32*-null mice (before the onset of demyelination), the localization of Caspr, Kv1.1 and Kv1.2 were not altered (Fig. 6). Similarly, it seemed plausible that the localization of Caspr or Kv1.2 might be altered in *Kv1.1*-null mice, but there was no obvious alteration in the localization of these proteins except that Kv1.2 staining was also seen in the nodal region, perhaps in the Schwann cell microvilli (Fig. 7).

Discussion

We found that the axonal proteins, Caspr, Kv1.1, Kv1.2, and Kv 2, are all localized in register with specializations of the myelin sheath, as shown schematically in Fig. 8. Caspr is localized to paranodal membrane; Kv1.1, Kv1.2, and Kv 2 are localized to the juxtaparanodal membrane. Along the internode, Caspr is found in the central strand, and Kv1.1/Kv1.2/Kv 2 in the flanking strands, of a tripartite strand apposing the inner mesaxon and the inner aspect of incisures. This organization is not disrupted in *Mag*-, *cx32*-, or *Kv1.1*-null mice, demonstrating that MAG, Cx32, and Kv1.1 are not essential for establishing or maintaining it. Thus, the myelin sheath leads to the molecular differentiation of the axonal membrane at paranodes, juxtaparanodes, and internodes.

VOLTAGE-SENSITIVE Na^+ CHANNELS AND ANKYRIN$_G$

The localizations of voltage-sensitive Na^+ channels, Kv1.1 and Kv1.2 ultimately depend on their linkage to the axonal cytoskeleton; otherwise, they would diffuse in the plane of the membrane. This linkage to the axonal cytoskeleton presumably requires protein-protein interactions within the same cell, or *cis*-interactions. How this occurs is best understood for voltage-sensitive Na^+ channels, which appear to be anchored to the cytoskeleton via ankyrin$_G$ (Shrager & Wu, 1994; Bennett *et al.*, 1997). Ankyrin$_G$ also binds, in *cis*, to neurofascin and Nr-CAM , which, in turn, may bind in *trans* to cell adhesion molecules on nodal microvilli of the myelinating Schwann cells (Raine, 1982; Ichimura & Ellisman, 1991; Bennett *et al.*, 1997). In addition, the cell adhesion molecules tenascin-C and tenascin-R may bind in *trans* to nodal voltage-gated Na^+ channels (Srinivasan *et al.*, 1998).

We confirmed that Caspr/paranodin is highly localized to paranodes, where it is thought to participate in the formation of axoglial junctions (Einheber *et al.*, 1997; Menegoz *et al.*, 1997; Bellen *et al.*, 1998). We have also directly demonstrated that the internodal localization of Caspr corresponds to the inner mesaxon of myelinating Schwann cells. This finding suggests that the putative molecule that binds to Caspr at paranodes may also localize Caspr at the inner mesaxon and at incisures, although the distinctive electron microscopic features of paranodal axoglial junctions have not been reported at the inner mesaxons or at incisures. Although MAG was an attractive candidate as the ligand for Caspr, the localization of Caspr, like voltage-sensitive Na^+ channels (Vabnick *et al.*, 1997), was not affected in *Mag*-null mice.

Caspr has a large extracellular domain, and is postulated to have a heterophilic binding partner in the

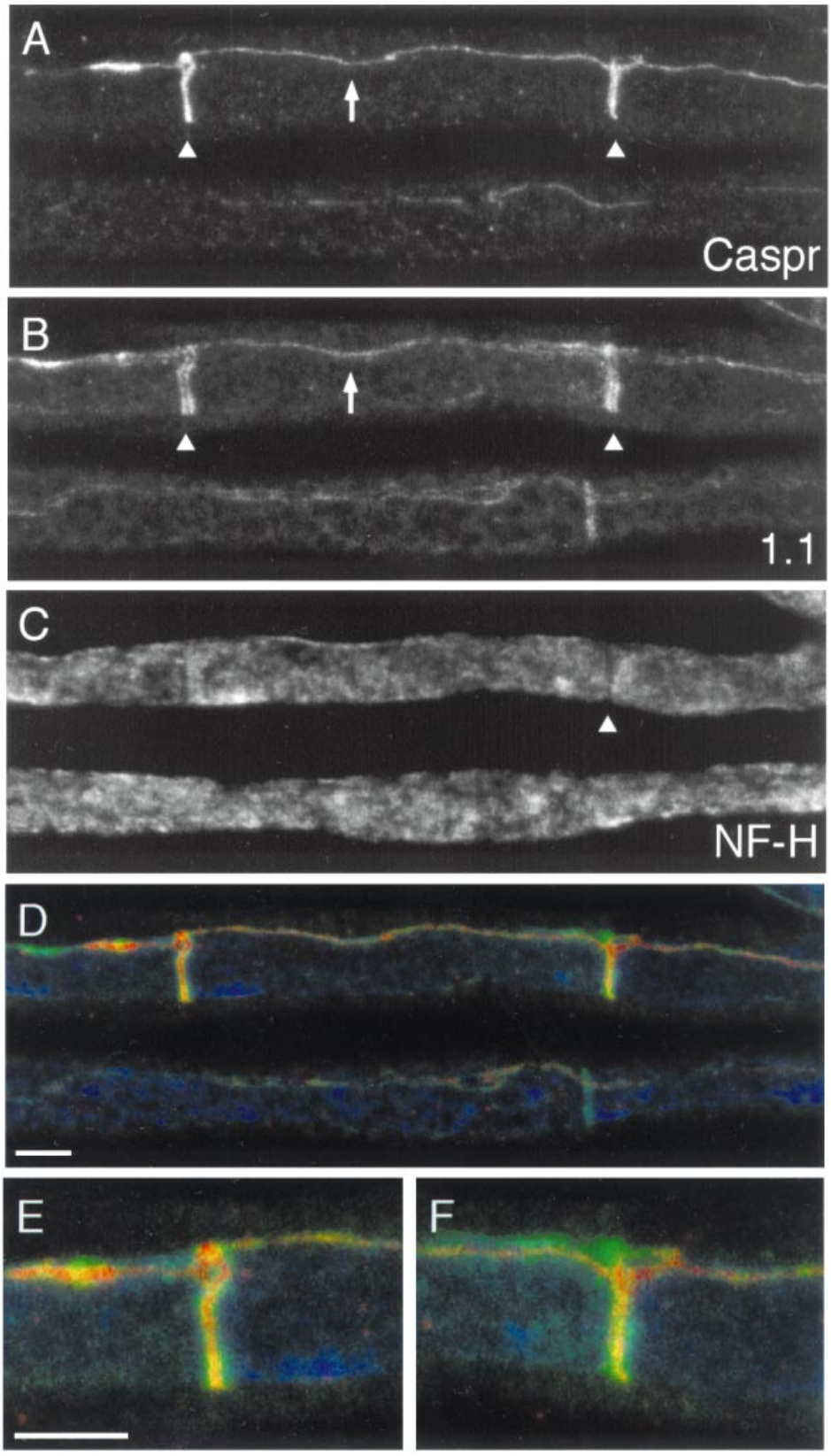

Fig. 4. Laser scanning confocal analysis of Caspr in the internodal region. These teased fibers were prepared from an adult mouse sciatic nerve following fixation for 30 minutes in paraformaldehyde, and labeling with a rabbit antiserum against Caspr, a mouse monoclonal antibody against Kv1.1, and a rat monoclonal antibody against NF-H, which were visualized with rhodamine-, fluorescein-, and cyanine 5-conjugated secondary antibodies, respectively. For clarity, the labeling from each antibody is shown separately in panels A-C; panels D–F show the merged images. Note the double line of Kv1.1 staining flanking the single line of Caspr staining, and the diminished NF-H staining at an incisure (small arrowhead). Scale bars: 5 m.

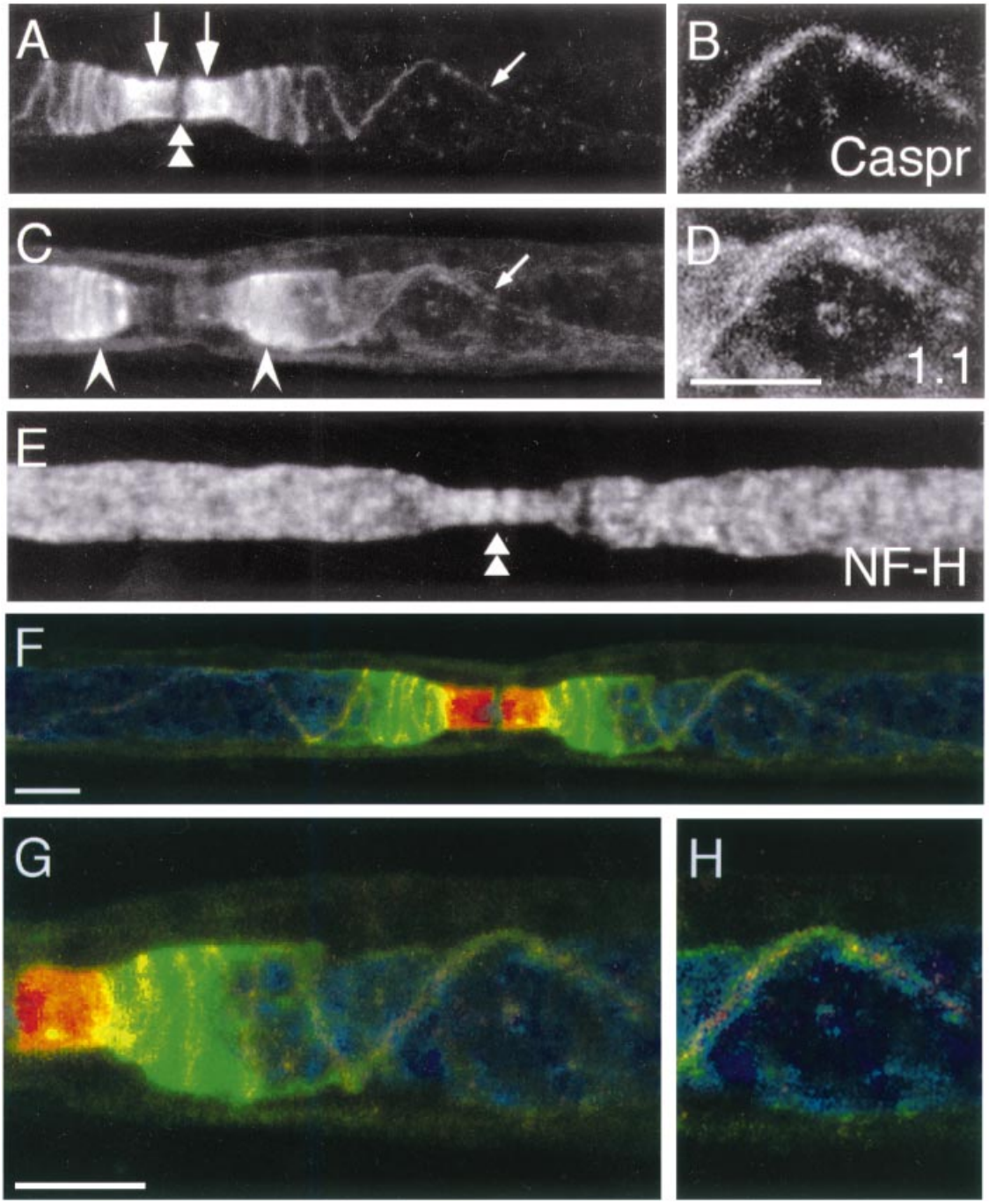

Fig. 5. Laser scanning confocal analysis of Caspr and Kv1.1 in the paranodal region. This teased fiber was prepared from an adult mouse sciatic nerve following fixation for 30 minutes in paraformaldehyde, and labeling with a rabbit antiserum against Caspr, a mouse monoclonal antibody against Kv1.1, and a rat monoclonal antibody against NF-H, which were visualized with rhodamine-, fluorescein-, and cyanine 5-conjugated secondary antibodies, respectively. For clarity, the labeling from each antibody is shown separately in panels A–E; panels G and H show the merged images. Panels B, D, G, and H have been enlarged to show better the immunostaining. Note the separation of Caspr and Kv1.1 staining at the paranode (large arrows) and juxtaparanode (large arrowheads), and that the spiral of Caspr staining in the juxtaparanodal region fills a void in the Kv1.1 staining. In the internodal region, the double line of Kv1.1 staining flanks the single line of Caspr staining. The NF-H staining is diminished at the node (double arrowheads). Scale bars: 5 m.

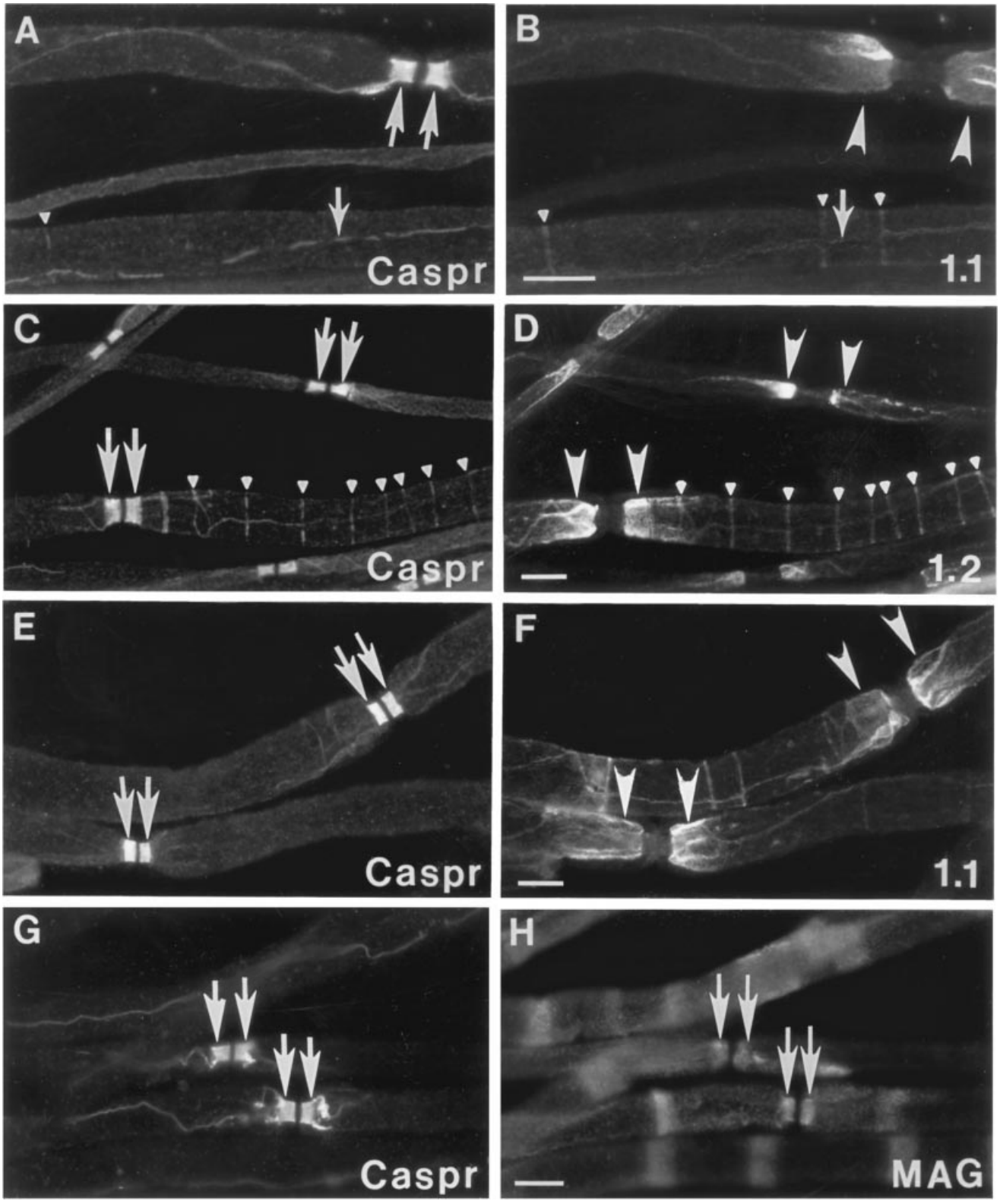

Fig. 6. The localization of Caspr, Kv1.1, Kv1.2 are not altered in myelinated fibers from *Mag*- or *cx*32-null mice. These are photomicrographs of teased fibers from young adult sciatic nerves, fixed Zamboni's fixative for 30 minutes, labeled with a rabbit antiserum against Caspr and a mouse monoclonal antibody against MAG, Kv1.1, or Kv1.2, and visualized in TRITC and FITC optics, respectively. Panels A–D are from *Mag*-null mice; panels E–H are from *cx*32-null mice. Note the normal pattern of Caspr-immunoreactivity at paranodes (large arrows), incisures (small arrowheads), and the inner mesaxon (small arrows). Scale bars: 10 m.

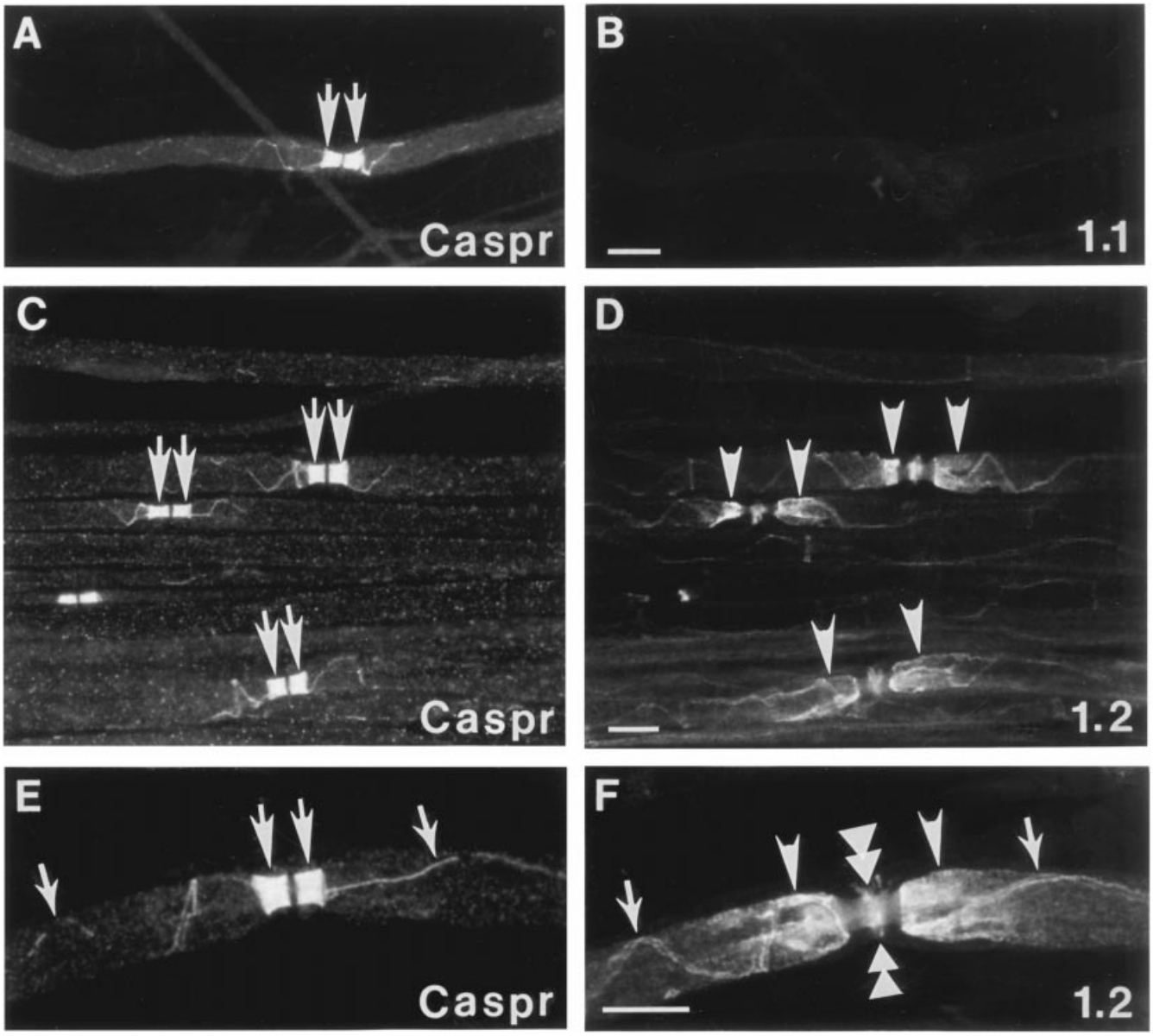

Fig. 7. The localization of Caspr, Kv1.1, Kv1.2 in myelinated fibers from *Kv1.1*- null mice. These are photomicrographs of teased fibers from P18 sciatic nerves, fixed Zamboni's for 60 minutes, labeled with a rabbit antiserum against Caspr and a mouse monoclonal antibody against MAG, Kv1.1, or Kv1.2, and visualized in TRITC and FITC optics, respectively. Note the normal pattern of Caspr-immunoreactivity at paranodes (large arrows) and the inner mesaxon (small arrows). Kv1.1-immunoreactivity is absent, and aberrant Kv1.2 staining in the nodal region of myelinating Schwann cells (double arrowheads). Scale bars: 10 m.

terminal loops of Schwann cells (Einheber *et al.*, 1997; Menegoz *et al.*, 1997; Bellen *et al.*, 1998). Caspr probably also interacts with axonal proteins. Electron microscopy reveals that the axonal cytoskeleton appears to be linked to the axonal membrane in the paranodal region (Ichimura & Ellisman, 1991). A *Drosophila* homologue of Caspr, neurexin IV, interacts with the Discs Lost, and mutations of *Discs Lost* result in the aberrant localization of neurexin IV (Bhat *et al.*, 1999). Discs Lost has multiple PDZ domains, one or more of which interact with the cytoplasmic PDZ-binding domain of neurexin IV. This is one of many examples of PDZ domains that cluster intrinsic membrane proteins (Craven & Bredt, 1998; Hata *et al.*, 1998). Caspr lacks a consensus PDZ-binding domain, however, so it remains to be determined how it is linked to the cytoskeleton.

Kv1.1, Kv1.2 AND Kv 2

The colocalization of Kv1.1, Kv1.2 and Kv 2 has been previously noted at juxtaparanodes (Wang *et al.*, 1993; Mi *et al.*, 1995; Rhodes *et al.*, 1997; Rasband *et al.*, 1998; Vabnick & Shrager, 1998; Vabnick *et al.*, 1999), and we have shown here that they are also co-localized at the

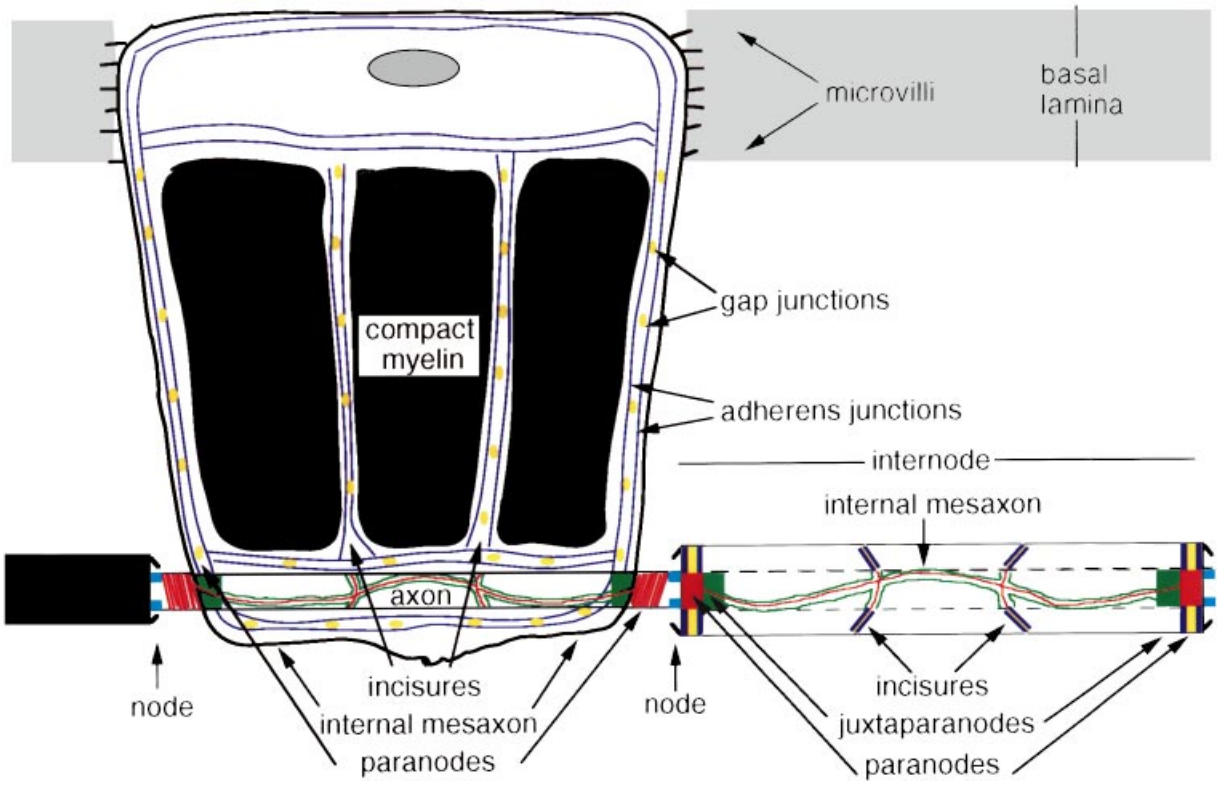

Fig. 8. Schematic view of a myelinated axon. One myelinating Schwann cell has been unrolled to reveal the regions that form compact myelin, the incisures, and the paranodes. Adherens junctions are depicted as two continuous lines (blue); these form a circumferential belt and are also found in the incisures. Gap junctions are depicted as ovals (yellow); these are found between the rows of adherens junctions. The localization of voltage-dependent Na^+ channels and ankyrin$_G$ (blue), Caspr (red), and Kv1.1/Kv1.2/Kv 2 (green) are indicated.

inner mesaxon and at incisures. Kv1.1 and Kv1.2 probably form heteromeric tetramers, the functional units of K^+ channels at all of these locations (Hopkins *et al.*, 1994). The association of Kv 2 with Kv1.1/Kv1.2 at juxtaparanodes results from direct protein-protein interactions (Rhodes *et al.*, 1997). The localization of Kv1.1 and Kv1.2 matches the locations of particle aggregates visualized by freeze-fracture electron microscopy at juxtaparanodes, the inner mesaxon, and at incisures in both the PNS and CNS (Rosenbluth 1976; Miller & Da Silva 1977; Stolinski *et al.*, 1981; Tao-Cheng & Rosenbluth, 1984; Stolinski *et al.*, 1985).

The localization of Kv1.1 and Kv1.2 in the juxtaparanodal region occurs in the absence of any anatomical evidence of bridges between the axon and myelin sheath, such as those seen at the node and paranode (Ichimura & Ellisman, 1991). Freeze-fracture electron microscopy, however, reveals juxtaparanodal particles in the adaxonal Schwann cell membrane (Miller & Da Silva, 1977; Stolinski *et al.*, 1981; Stolinski *et al.*, 1985), possibly the "paranodal" K^+ channels that have been identified electrophysiologically (Chiu, 1991). Intramembranous particles with similar characteristics to these juxtaparanodal particles are found in the Schwann cell membrane at the internal mesaxon and apposing incisures (Stolinski *et al.*, 1985). Thus, there may be a K^+ channel in the Schwann cell membrane apposing the axonal Kv1.1 and Kv1.2 channels, but whether trans-interactions between these putative channels serve to localize Kv1.1/Kv1.2 remains to be determined.

Kv1.1 and Kv1.2 are *Shaker*-type channels, and along other members of their gene family, are widely expressed in the brain, with diverse subcellular localizations (Sheng *et al.*, 1994; Wang *et al.*, 1994; Veh *et al.*, 1995; Rhodes *et al.*, 1997). Whether PDZ-containing proteins link Kv1.1 and Kv1.2 to the axonal cytoskeleton, as they do at synapses (Kim *et al.*, 1995; Topinka & Bredt, 1998), remains to be determined, but one PDZ protein, PSD95, is a promising candidate, as it is known to cluster *Shaker*-type channels (Kim *et al.*, 1995). In *Drosophila*, a PDZ-containing protein called Discs Large is necessary for *Shaker* channels to be to localized at the neuromuscular junction (Tejedor *et al.*, 1997). The tripartite organization of Caspr and Kv1.1/Kv1.2 suggests the possibility that an adaptor protein interacts with both Caspr and Kv1.1 and/or Kv1.2. Caspr could be localized to the internodal membrane by a *trans*-interaction with a protein expressed by the myelinating

Schwann cell, and recruit Kv1.1 and/or Kv1.2 by *cis*-interactions.

Acknowledgments

This work was supported by the NIH (NS08075, NS37100, and NS34528 to S.S.S., and RO1-23375 to S.Y.C. and A.M.), We thank Drs. Vann Bennett, David Colman, Elliot Hertzberg, Virginia Lee, S. Rock Levinson, James Salzer, James Trimmer for their generous gifts of antibodies, and Dr. Klaus Willecke for the *cx32*-null mice.

References

BALICE-GORDON, R. J., BONE, L. J. & SCHERER, S. S. (1998) Functional gap junctions in the Schwann cell myelin sheath. *Journal of Cell Biology* **142**, 1095–1104.

BELLEN, H. J., LU, Y., BECKSTEAD, R. & BHAT, M. A. (1998) Neurexin IV, Caspr and paranodin—novel members of the neurexin family: encounters of axons and glia. *Trends in Neurosciences* **21**, 444–449.

BENNETT, V., LAMBERT, S., DAVIS, J. Q. & ZHANG, X. (1997) Molecular architecture of the specialized axonal membrane at the node of Ranvier. *Society of General Physiology* **52**, 107–120.

BERTHOLD, C.-H. & RYDMARK, M. (1995) Morphology of normal peripheral axons. In *The Axon* (edited by WAXMAN, S. G., KOCSIS, J. D. & STYS, P. K.), pp. 13–48. New York: Oxford University Press.

BHAT, M. A., IZADDOOST, S., LU, Y., CHO, K. O., CHOI, K. W. & BELLEN, H. J. (1999) Discs Lost, a novel multi-PDZ domain protein, establishes and maintains epithelial polarity. *Cell* **96**, 833–845.

CHIU, S. Y. (1991) Functions and distribution of voltage-gated sodium and potassium channels in mammalian Schwann cells. *Glia* **4**, 541–558.

CHIU, S. Y., SCHERER, S. S., BLONSKI, M., KANG, S. S. & MESSING, A. (1994) Axons regulate the expression of Shaker potassium channel genes in Schwann cells in peripheral nerve. *Glia* **12**, 1–11.

CHIU, S. Y., ZHOU, L., ZHANG, C.-L. & MESSING, A. (1999) Analysis of potassium channel functions in mammalian axons by gene knockouts. *Journal of Neurocytology* **28**, 349–364.

CRAVEN, S. E. & BREDT, D. S. (1998) PDZ proteins organize synaptic signaling pathways. *Cell* **93**, 495–498.

EINHEBER, S., ZANAZZI, G., CHING, W., SCHERER, S. S., MILNER, T. A., PELES, E. & SALZER, J. L. (1997) The axonal membrane protein Caspr/Neurexin IV is a component of the septate-like paranodal junctions that assemble during myelination. *Journal of Cell Biology* **139**, 1495–1506.

ELLISMAN, M. H. & LEVINSON, S. R. (1982) Immunocytochemical localization of sodium channel distributions in the excitable membranes of *Electrophorus electricus*. *Proceedings of the National Academy of Sciences USA* **79**, 6707–6711.

FANNON, A. M., SHERMAN, D. L., ILYINA-GRAGEROVA, G., BROPHY, P. J., FRIEDRICH, V. L. & COLMAN, D. R. (1995) Novel E-cadherin mediated adhesion in peripheral nerve: Schwann cell architecture is stabilized by autotypic adherens junctions. *Journal of Cell Biology* **129**, 189–202.

FRIEDE, R. L. & SAMORAJSKI, T. (1969) The clefts of Schmidt-Lantermann: A quantitative electron microscopic study of their structure in developing adult sciatic nerves of the rat. *Anatomical Record* **165**, 89–102.

GILLESPIE, C. S., SHERMAN, D. L., BLAIR, G. E. & BROPHY, P. J. (1994) Periaxin, a novel protein of myelinating Schwann cells with a possible role in axonal ensheathment. *Neuron* **12**, 497–508.

HAIMOVICH, B., BONILLA, E., CASADEI, J. & BARCHI, R. L. (1984) Immunocytochemical localization of the mammalian voltage-dependent sodium channel using polyclonal antibodies against the purified protein. *Journal of Neuroscience* **4**, 2259–2268.

HATA, Y., NAKANISHI, H. & TAKAI, Y. (1998) Synaptic PDZ domain-containing proteins. *Neuroscience Research* **32**, 1–7.

HIRANO, A. & LLENA, J. F. (1995) Morphology of central nervous system axons. In *The Axon* (edited by WAXMAN, S. G., KOCSIS, J. D. & STYS, P. K.), pp. 49–67. New York: Oxford University Press.

HOPKINS, W. F., ALLEN, M. L., MOUAMED, K. M. & TEMPEL, B. L. (1994) Properties of voltage-gated K^+ currents expressed in Xenopus oocytes by mKv1.1, mKv1.2 and their heteromultimers as revealed by mutagenesis of the dendrotoxin-binding site in Kv1.1. *Pflügers Archives* **428**, 382–390.

ICHIMURA, T. & ELLISMAN, M. H. (1991) Three-dimensional fine structure of cytoskeletal-membrane interactions at nodes of Ranvier. *Journal of Neurocytology* **20**, 667–681.

KIM, E., NIETHAMMER, M., ROTHSCHILD, A., JAN, Y. N. & SHENG, M. (1995) Clustering of Shaker-type K^+ channels by interaction with a family of membrane-associated guanylate kinases. *Nature* **378**, 85–88.

LAMBERT, S., DAVIS, J. Q. & BENNETT, V. (1997) Morphogenesis of the node of Ranvier: co-clusters of ankyrin and ankyrin-binding integral proteins define early developmental intermediates. *Journal of Neuroscience* **17**, 7025–7036.

LEE, V., WU, H. L. & SCHLAEPFER, W. W. (1982) Monoclonal antibodies recognized individual neurofilament triplet proteins. *Proceedings of the National Academy of Sciences USA* **79**, 6089–6092.

LI, C., TOPAK, M. B., GERIAL, R., CALPOFF, S., ABRAMOW-NEWERLY, W., TRAPP, B., PETERSON, A. & RODER, J. (1994) Myelination in the absence of myelin-associated glycoprotein. *Nature* **369**, 747–750.

LI, C., TRAPP, B., LUDWIN, S., PETERSON, A. & RODER, J. (1998) Myelin associated glycoprotein modulates glia-axon contact in vivo. *Journal of Neuroscience Research* **51**, 210–217.

MARTINI, R. & SCHACHNER, M. (1988) Immunoelectron microscopic localization of neural cell adhesion molecules (L1, N-CAM, and myelin-associated glycoprotein) in regenerating adult mouse sciatic nerve. *Journal of Cell Biology* **106**, 1735–1746.

MATA, M., KUPINA, N. & FINK, D. J. (1992) Phosphorylation-dependent neurofilament epitopes are reduced at the node of Ranvier. *Journal of Neurocytology* **21**, 199–210.

MENEGOZ, M., GASPAR, P., LE BERT, M., GALVEZ, T., BURGAYA, F., PALFREY, C., EZAN, P., ARNOS, F. & GIRAULT, J.-A. (1997) Paranodin, a glycoprotein of neuronal paranodal membranes. *Neuron* **19**, 319–331.

MI, H. Y., DEERINCK, T. J., ELLISMAN, M. H. & SCHWARZ, T. L. (1995) Differential distribution of closely related potassium channels in rat Schwann cells. *Journal of Neuroscience* **15**, 3761–3774.

MILLER, R. G. & DA SILVA, P. P. (1977) Particle rosettes in the periaxonal Schwann cell membrane and particle clusters in the axolemma of rat sciatic nerve. *Brain Research* **130**, 135–141.

MONTAG, D., GIESE, K. P., BARTSCH, U., MARTINI, R., LANG, Y., BLUTHMANN, H., KARTHIGASAN, J., KIRSCHNER, D. A., WINTERGERST, E. S., NAVE, K.-A., ZIELASEK, J., TOYKA, K. V., LIPP, H.-P. & SCHACHNER, M. (1994) Mice deficient for the myelin-associated glycoprotein show subtle abnormalities in myelin. *Neuron* **13**, 229–246.

NELLES, E., BUTZLER, C., JUNG, D., TEMME, A., GABRIEL, H.-D., DAHL, U., TRAUB, O., STUMPEL, F., JUNGERMANN, K., ZIELASEK, J., TOYKA, K. V., DERMIETZEL, R. & WILLECKE, K. (1996) Defective propagation of signals generated by sympathetic nerve stimulation in the liver of connexin32-deficient mice. *Proceedings of the National Academy of Sciences USA* **93**, 9565–9570.

PEDRAZA, L., OWENS, G. C., GREEN, L. A. D. & SALZER, J. L. (1990) The myelin-associated glycoproteins: membrane disposition, evidence of a novel disulfide linkage between immunoglobulin-like domains, and posttranslational palmitylation. *Journal of Cell Biology* **111**, 2651–2661.

PELES, E., NATIV, M., LUSTIG, M., GRUMET, M., MARTINEZ, R., PLOWMAN, G. D. & SCHLESSINGER, J. (1997) Identification of a novel contactin-associated transmembrane receptor with multiple domains implicated in protein-protein interactions. *European Molecular Biology Organization Journal* **16**, 978–988.

PETERS, A., PALAY, S. L. & WEBSTER, H. D. (1991) *The Fine Structure of the Nervous System*. New York: Oxford University Press.

RAINE, C. S. (1982) Differences between the nodes of Ranvier of large and small diameter fibres in the P.N.S. *Journal of Neurocytology* **11**, 935–947.

RASBAND, M., TRIMMER, J. S., SCHWARZ, T. L., LEVINSON, S. R., ELLISMAN, M. H., SCHACHNER, M. & SHRAGER, P. (1998) Potassium channel distribution, clustering, and function in remyelinating rat axons. *Journal of Neuroscience* **18**, 36–47.

RHODES, K. J., STRASSLE, B. W., MONAGHAN, M. M., BEKELE-ARCURI, Z., MATOS, M. F. & TRIMMER, J. S. (1997) Association and colocalization of the Kv 1 and Kv 2 in with Kv1 -subunits in mammalian brain K^+ channel complexes. *Journal of Neuroscience* **17**, 8646–8258.

ROSENBLUTH, J. (1976) Intramembranous particle distribution at the node of Ranvier and adjacent axolemma in myelinated axons of the frog brain. *Journal of Neurocytology* **5**, 731–745.

ROSENBLUTH, J. (1988) Role of glial cells in the differentiation and function of myelinated axons. *International Journal of Developmental Neuroscience* **6**, 3–24.

SALZER, J. L. (1997) Clustering sodium channels at the node of Ranvier: Close encounters of the axon-glia kind. *Neuron* **18**, 843–846.

SCHERER, S. S. (1996) Molecular specializations at nodes and paranodes in peripheral nerve. *Microscopy Research and Technique* **34**, 452–461.

SCHERER, S. S., XU, Y.-T., NELLES, E., FISCHBECK, K., WILLECKE, K. & BONE, L. J. (1998) Connexin32-null mice develop a demyelinating peripheral neuropathy. *Glia* **24**, 8–20.

SHENG, M., TSAUR, M.-L., JAN, Y. N. & JAN, L. Y. (1994) Contrasting subcellular localization of the Kv1.2 K^+ channel subunit in different neurons of rat brain. *Journal of Neuroscience* **14**, 2408–2417.

SHRAGER, P. & WU, J. V. (1994) Ionic channels of myelinated axons. In *Handbook of Membrane Channels*, pp. 105–113. Academic Press.

SMALL, J. R., GHABRIEL, M. N. & ALLT, G. (1987) The development of Schmidt-Lanterman incisures: an electron microscope study. *Journal of Anatomy* **150**, 277–286.

SMART, S. L., LOPANTSEV, V., ZHANG, C. L., ROBBINS, C. A., WANG, H., CHIU, S. Y., SCHWARTZKROIN, P. A., MESSING, A. & TEMPEL, B. L. (1998) Deletion of the Kv1.1 potassium channel causes epilepsy in mice. *Neuron* **20**, 809–819.

SRINIVASAN, Y., SCHACHNER, M. & CATTERALL, W. (1998) Interaction of voltage-gated sodium channels with the extracellular matrix moleculres tenascin-C and tenascin-R. *Proceedings of the National Academy of Sciences USA* **95**, 15753–15757.

STOLINSKI, C., BREATHNACH, A. S., MARTIN, B., THOMAS, P. K., KING, R. M. H. & GABRIEL, G. (1981) Associated particle aggregates in juxtaparanodal axolemma and adaxonal Schwann cell membrane of rat peripheral nerve. *Journal of Neurocytology* **10**, 679–691.

STOLINSKI, C., BREATHNACH, A. S., THOMAS, P. K., GABRIEL, G. & KING, R. M. H. (1985) Distribution of particle aggregates in the internodal axolemma and adaxonal Schwann cell membrane of rodent peripheral nerve. *Journal of the Neurological Sciences* **67**, 213–222.

TAO-CHENG, J.-H. & ROSENBLUTH, J. (1984) Extranodal particle accumulations in the axolemma of myelinated frog optic axons. *Brain Research* **308**, 289–300.

TEJEDOR, F. J., BOKHARI, A., ROGERO, O., GORCZYCA, M., ZHANG, J., KIM, E., SHENG, M. & BUDNIK, V. (1997) Essential role for dlg in synaptic clustering of *Shaker* K^+ channels *in vivo*. *Journal of Neuroscience* **17**, 152–159.

TOPINKA, J. R. & BREDT, D. S. (1998) N-terminal palmitoylation of PSD-95 regulates association with cell membranes and interaction with K^+ channel Kv1.4. *Neuron* **20**, 125–134.

TRAPP, B. D. & QUARLES, R. H. (1982) Presence of the myelin-associated glycoprotein correlates with alterations in the periodicity of peripheral myelin. *Journal of Cell Biology* **92**, 877–882.

VABNICK, I., MESSING, A., CHIU, S. Y., LEVINSON, S. R., SCHACHNER, M., RODER, J., LI, C. M., NOVAKOVIC, S. & SHRAGER, P. (1997) Sodium channel distribution in axons of hypomyelinated and MAG null mutant mice. *Journal of Neuroscience Research* **50**, 321–336.

VABNICK, I. & SHRAGER, P. (1998) Ion channel redistribution and function during development of the myelinated axon. *Journal of Neurobiology* **37**, 80–96.

VABNICK, I., TRIMMER, J. S., SCHWARZ, T. L., LEVINSON, S. R., RISAL, D. & SHRAGER, P. (1999) Dynamic potassium channel distributions during axonal development prevent aberrant firing patterns. *Journal of Neuroscience* **19**, 747–758.

VEH, R. W., LICHTINGHAGEN, R., SEWING, S., WUNDER, F., GRUMBACH, I. M. & PONGS, O. (1995) Immunohistochemical localization of five members of the Kv1 channel subunits: contrasting subcellular locations and neuron-specific co-localizations in rat brain. *European Journal of Neuroscience* **7**, 2189–2205.

WANG, H., KUNKEL, D. D., MARTIN, T. M., SCHWARTKROIN, P. A. & TEMPEL, B. L. (1993) Heteromultimeric K^+ channels in terminal and juxtaparanodal regions of neurons. *Nature* **365**, 75–79.

WANG, H., KUNKEL, D. D., SCHWARTZKROIN, P. A. & TEMPEL, B. L. (1994) Localization of Kv1.1 and Kv1.2, two K channel proteins, to synaptic terminals, somata, and dendrites in the mouse brain. *Journal of Neuroscience* **14**, 4588–4599.

YIN, X. H., CRAWFORD, T. O., GRIFFIN, J. W., TU, P. H., LEE, V. M. Y., LI, C. M., RODER, J. & TRAPP, B. D. (1998) Myelin-associated glycoprotein is a myelin signal that modulates the caliber of myelinated axons. *Journal of Neuroscience* **18**, 1953–1962.

ZAMBONI, L. & DE MARTINO, C. (1967) Buffered picric-acid formaldehyde: a new rapid fixative for electron-microscopy. *Journal of Cell Biology* **35**, 148A.

ZHOU, L., ZHANG, C. L., MESSING, A. & CHIU, S. Y. (1998) Temperature-sensitive neuromuscular transmission in Kv1.1 null mice: Role of potassium channels under the myelin sheath in young nerves. *Journal of Neuroscience* **18**, 7200–7215.